

Self-Correcting Bayesian Optimization through Bayesian Active Learning

Carl Hvarfner¹ Erik Hellsten¹ Frank Hutter^{2,3} Luigi Nardi^{1,4,5}

Abstract

Gaussian processes are cemented as the model of choice in Bayesian optimization and active learning. Yet, they are severely dependent on cleverly chosen hyperparameters to reach their full potential, and little effort is devoted to finding the right hyperparameters in the literature. We demonstrate the impact of selecting good hyperparameters for GPs and present two acquisition functions that explicitly prioritize this goal. Statistical distance-based Active Learning (SAL) considers the average *disagreement* among samples from the posterior, as measured by a statistical distance. It is shown to outperform the state-of-the-art in Bayesian active learning on a number of test functions. We then introduce Self-Correcting Bayesian Optimization (SCoReBO), which extends SAL to perform Bayesian optimization and active hyperparameter learning simultaneously. SCoReBO learns the model hyperparameters at improved rates compared to vanilla BO, while outperforming the latest Bayesian optimization methods on traditional benchmarks. Moreover, the importance of self-correction is demonstrated on an array of exotic Bayesian optimization tasks.

1. Introduction

Bayesian Optimization (BO) is an elegant and powerful paradigm to optimize black-box problems, i.e., problems that can only be accessed by point-wise function evaluations. This problem class encompasses a large number of real-life optimization tasks, including drug discovery (Griffiths & Hernández-Lobato, 2017), material design (Frazier & Wang, 2016; Zhang et al., 2020), configuration of combinatorial problem solvers (Hutter et al., 2011; 2017), hardware design (Ejeh et al., 2022; Nardi et al., 2019), hyperparameter tuning (Hvarfner et al., 2022b; Kandasamy et al., 2018; Ru

*Equal contribution ¹Lund University ²University of Freiburg ³Bosch Center for Artificial Intelligence ⁴Stanford University ⁵DBTune. Correspondence to: Carl Hvarfner <carl.hvarfner@cs.lth.se>.

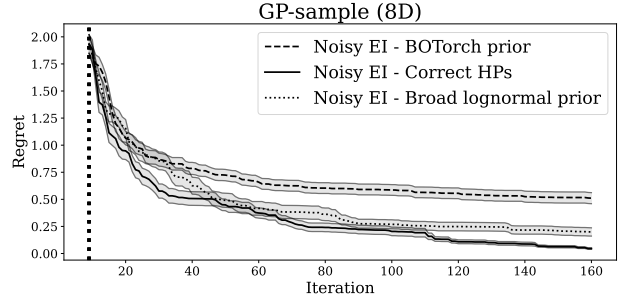


Figure 1. Simple regret using true hyperparameters (filled) versus BOTorch (dotted) and a wide log-normal prior (dashed). The BO results are averaged over 20 runs of different functions drawn from a GP with fixed lengthscales and the EI acquisition function.

et al., 2020) including reinforcement learning agents such as AlphaGo (Chen et al., 2018), and robotics (Berkenkamp et al., 2021; Calandra et al., 2014; Mayr et al., 2022a;b).

Gaussian processes (GPs) with stationary kernels are a popular choice as surrogate models in BO applications. Given a data set, the model hyperparameters are typically estimated using either Maximum Likelihood Estimation (MLE) or Maximum a Posteriori estimation (MAP) (Rasmussen & Williams, 2006). Alternatively, a fully Bayesian treatment of the model hyperparameters (Osborne, 2010; Snoek et al., 2012) removes the need to choose a particular set of values through Monte Carlo integration. However, little work is dedicated to understanding the relationship between the GP hyperparameters and the BO performance, and hyperparameter uncertainty is not considered by any prevalent BO acquisition function. In contrast, the field of Bayesian Active Learning (BAL) has a collection of acquisition functions (Houlsby et al., 2011; Riis et al., 2022) based solely on reducing hyperparameter-induced measures of uncertainty.

The importance of the GP hyperparameters in BO is illustrated in Fig. 1, where the average simple regret over 20 optimization runs of 8-dimensional functions drawn from a Gaussian process prior is shown. The curves correspond to the performance of the noisy EI (Jones et al., 1998; Letham et al., 2018) acquisition function under fully Bayesian hyperparameter treatment for two prevalent hyperparameter priors, as well as the performance when the correct model hyperparameters are used. Clearly, good model hyperpa-

rameters have substantial impact on BO performance under a conventional setup, and BO methods could benefit from estimating the model hyperparameters accurately. Furthermore, the hyperparameter estimation task can quickly become insurmountable under exotic problem setups, including heterogeneity in the objective function (Cowen-Rivers et al., 2020; Eriksson et al., 2019; Snoek et al., 2014; Wan et al., 2021), high-dimensional search spaces (Eriksson & Jankowiak, 2021; Papenmeier et al., 2022), and additively decomposable objectives (Gardner et al., 2017; Kandasamy et al., 2015). The complexity of such problems warrants the use of more complex, task-specific surrogate models. Under these setups, the ultimate success of the optimization increasingly hinges on the presumed accuracy of the task-specific surrogate.

We proceed in two steps. We first introduce *Statistical distance-based Active Learning* (SAL), which improves Bayesian active learning by generalizing previous work (Riis et al., 2022) and introducing a more holistic measure of disagreement between the marginal posterior predictive distribution and each conditional posterior predictive distribution. By considering the hyperparameter-induced disagreement between models in the acquisition function, the learning of model hyperparameters is accelerated. We then propose *Self-Correcting Bayesian Optimization* (SCoreBO), which builds upon SAL by explicitly learning the location of the optimizer in conjunction with conventional model hyperparameters. This achieves accelerated hyperparameter learning and yields improved optimization performance on both conventional and exotic BO tasks. Moreover, SCoreBO demonstrates robustness to suboptimal hyperparameter priors. Formally, We make the following contributions:

1. We introduce SAL, a novel and efficient acquisition function for Bayesian active learning based on statistical distances (Sec. 3.1)
2. We introduce SCoreBO, the first acquisition function for joint BO and hyperparameter learning (Sec. 3.2).
3. We show competitive performance on an array of conventional AL (Sec. 4.1) and BO tasks (Sec. 4.2).
4. We demonstrate SCoreBO on exotic BO settings (Sec. 4.3), highlighting the ability of the method to enhance SAASBO (Eriksson & Jankowiak, 2021) and AddGP (Kandasamy et al., 2015).

2. Background

In this section, we introduce Gaussian processes, and Bayesian treatment of hyperparameters through Monte Carlo integration. Thereafter, we cover Bayesian optimization, Bayesian active learning, and statistical distances.

2.1. Gaussian processes

Gaussian processes (GPs) has become the model class of choice in most BO and active learning applications. It provides a distribution over functions $f \sim \mathcal{GP}(m(\cdot), k(\cdot, \cdot))$ fully defined by the mean function $m(\cdot)$ and the covariance function $k(\cdot, \cdot)$. Under this distribution, the value of the function $f(\mathbf{x})$, at a given point \mathbf{x} , is normally distributed with a closed-form solution for the mean and variance. We assume that observations are perturbed by Gaussian noise, such that $y_{\mathbf{x}} = f(\mathbf{x}) + \varepsilon$, $\varepsilon^2 \sim N(0, \sigma_{\varepsilon}^2)$. We also assume the mean function to be constant, such that the dynamics are fully determined by the covariance function $k(\cdot, \cdot)$.

To account for differences in variable importance, each dimension is individually scaled using lengthscale hyperparameters ℓ_i . For D -dimensional inputs \mathbf{x} and \mathbf{x}' , the distance $r(\mathbf{x}, \mathbf{x}')$ is subsequently computed as $r^2 = \sum_{i=1}^D (x_i - x'_i)^2 / \ell_i^2$. Along with the outputscale σ_f , the set $\theta = \{\ell, \sigma_{\varepsilon}, \sigma_f\}$ comprise the set of hyperparameters that are conventionally learned.

2.2. Distributions over GP hyperparameters

The likelihood surface for the GP hyperparameters is typically highly multi-modal (Rasmussen & Williams, 2006; Yao et al., 2020), where different modes represent different bias-variance trade-offs (Rasmussen & Williams, 2006; Riis et al., 2022). To avoid having to choose a single mode, one can define a prior $p(\theta)$ and then marginalize with respect to the hyperparameters when performing predictions. The posterior probability of observing a value $y_{\mathbf{x}}$ for a point \mathbf{x} is given by (Lalchand & Rasmussen, 2020):

$$p(y_{\mathbf{x}}|\mathcal{D}) = \int_{\theta} \int_f p(y_{\mathbf{x}}|f, \theta) p(f|\theta, \mathcal{D}) p(\theta|\mathcal{D}) df d\theta, \quad (1)$$

where \mathcal{D} is the observed data. The inner integral is equal to the GP predictive posterior,

$$\int_f p(y_{\mathbf{x}}|f, \theta) p(f|\theta, \mathcal{D}) df = p(y_{\mathbf{x}}|\theta) = \mathcal{N}(\mu_{\mathbf{x}}, \Sigma_{\mathbf{x}}), \quad (2)$$

where the predictive mean and covariance are computed as

$$\begin{aligned} \mu_{\mathbf{x}} &= K_{\theta}^* (K_{\theta} + \sigma_n^2 \mathbb{I})^{-1} \bar{\mathbf{y}} \\ \Sigma_{\mathbf{x}} &= K_{\theta}^{**} - K_{\theta}^* (K_{\theta} + \sigma_n^2 \mathbb{I})^{-1} K_{\theta}^*, \end{aligned}$$

and where

$$\begin{bmatrix} K_{\theta} & K_{\theta}^* \\ K_{\theta}^* & K_{\theta}^{**} \end{bmatrix} \quad (3)$$

is the parameterized kernel matrix and \mathbf{y} are the previously observed values. However, the outer integral is intractable and is estimated using Markov Chain Monte Carlo (MCMC)

methods. The resulting posterior prediction

$$p(y_{\mathbf{x}}|\mathcal{D}) = \int_{\boldsymbol{\theta}} p(y_{\mathbf{x}}|\mathcal{D}, \boldsymbol{\theta})p(\boldsymbol{\theta}|\mathcal{D})d\boldsymbol{\theta} \quad (4)$$

$$\approx \frac{1}{M} \sum_{j=1}^M p(y_{\mathbf{x}}|\mathcal{D}, \boldsymbol{\theta}_j), \quad \boldsymbol{\theta}_j \sim p(\boldsymbol{\theta}_j|\mathcal{D}), \quad (5)$$

is a Gaussian Mixture Model (GMM).

2.3. Bayesian Optimization

Bayesian Optimization (BO) is the problem of maximizing a black-box function f over a compact domain \mathcal{X} ,

$$\max_{\mathbf{x} \in \mathcal{X}} f(\mathbf{x}), \quad (6)$$

such that f can only be sampled point-wise through expensive, noisy evaluations $y_{\mathbf{x}} = f(\mathbf{x}) + \varepsilon$, where $\varepsilon \sim \mathcal{N}(0, \varepsilon^2)$. New configurations are chosen by optimizing an *acquisition function*, which uses the surrogate model to quantify the utility of evaluating new points in the search space. Examples of such heuristics are Expected Improvement (EI) (Jones et al., 1998) and Upper Confidence Bound (UCB) (Srinivas et al., 2012). More sophisticated look-ahead approaches include Knowledge Gradient (KG) (Frazier, 2018) as well as a class of particular importance for our approach, which is the information-theoretic acquisition function class. These acquisition functions consider a mutual information objective to select the next query,

$$\alpha_{\text{MI}}(\mathbf{x}) = I(y_{\mathbf{x}}; * | \mathcal{D}_n) \quad (7)$$

where $*$ can entail either the optimum \mathbf{x}^* as in (Predictive) Entropy Search (ES/PES) (Hennig & Schuler, 2012b; Hernández-Lobato et al., 2014), the optimal value f^* as in Max-value Entropy Search (MES) (Moss et al., 2021; Takeno et al., 2020; Wang & Jegelka, 2017) or the tuple (\mathbf{x}^*, f^*) , used in Joint Entropy Search (JES) (Hvarfner et al., 2022a; Tu et al., 2022). FITBO (Ru et al., 2018) has similarities to our work, in that it considers a MES-like objective, where the optimal value is governed by a hyperparameter of a transformed GP.

2.4. Bayesian Active Learning

In contrast to BO, which aims to find a maximizer to an unknown function, Active Learning (AL) (Settles, 2009) seeks to accurately learn the black-box function globally. Thus, the objective is to minimize the expected prediction loss. Typically, AL acquisition functions are either decision-theoretic or information-theoretic. The former category minimizes the prediction loss over some validation set, whereas the latter minimizes the space of plausible models given the observed data (Houlsby et al., 2011; MacKay, 1992).

Among the decision theoretic acquisition functions, the most common is the *Integrated Mean Squard Prediction Error* (IMSPE) (Cohn, 1996), which for GP models equals the integrated posterior variance (Binois et al., 2019). In the information-theoretic category, *Active Learning McKay* (ALM) (MacKay, 1992) is the most straight-forward. It selects the point with the highest Shannon Entropy, which for GPs amounts to selecting the point with the highest variance. This can further be extended to Bayesian ALM (BALM), where Monte Carlo integration is performed over the hyperparameters.

Bayesian Active Learning by Disagreement (BALD) (Houlsby et al., 2011) was among the first Bayesian active learning approaches to focus on learning the model hyperparameters. It approximates the reduction in entropy over the GP hyperparameters from observing a new data point and was later extended to work for deep Bayesian active learning (Kirsch et al., 2019).

Lastly, Riis et al. (2022) propose a *Bayesian Query-by-Committee* (BQBC) acquisition function. BQBC queries the point where the variance V of the GP mean is the largest, with respect to changing model hyperparameters:

$$\alpha_{\text{BQBC}}(\mathbf{x}) = V_{\boldsymbol{\theta}}[\boldsymbol{\mu}_{\boldsymbol{\theta}}(\mathbf{x})] \quad (8)$$

$$= \mathbb{E}_{\boldsymbol{\theta}}[(\boldsymbol{\mu}_{\boldsymbol{\theta}}(\mathbf{x}) - \bar{\boldsymbol{\mu}}(\mathbf{x}))^2]. \quad (9)$$

where $\bar{\boldsymbol{\mu}}(\mathbf{x})$ is the marginal mean at (\mathbf{x}) . As such, BQBC queries at the location which maximizes the distance between the marginal posterior and the conditionals according to some distance metric (the posterior mean), henceforth referred to as hyperparameter-induced *posterior disagreement*. However, disagreement in mean alone does not incentivize exploration. Thus, (Riis et al., 2022) also present *Query-by-Mixture of Gaussian Processes* (QBMGP), adds the BALM criterion to the BQBC acquisition function.

2.5. Statistical Distances

A statistical distance quantifies the distance between two statistical objects. We focus on two proper metrics, which have closed forms for Gaussian random variables.

The Hellinger distance is a similarity measure between two probability distributions which has previously been employed in the context of BO-driven automated model selection by Malkomes et al. (2016). For two probability distributions p and q , it is defined as

$$H^2(p, q) = \frac{1}{2} \int_{\mathcal{X}} \left(\sqrt{p(x)} - \sqrt{q(x)} \right)^2 \lambda dx, \quad (10)$$

with some auxiliary measure λ with which both p and q are absolutely continuous. Specifically, for two normally

distributed variables $z_1 \sim \mathcal{N}(\mu_1, \sigma_1^2)$, $z_2 \sim \mathcal{N}(\mu_2, \sigma_2^2)$,

$$H^2(z_1, z_2) = 1 - \sqrt{\frac{2\sigma_1\sigma_2}{\sigma_1^2 + \sigma_2^2}} \exp\left[-\frac{1}{4} \frac{(\mu_1 - \mu_2)^2}{\sigma_1^2 + \sigma_2^2}\right]. \quad (11)$$

The Wasserstein distance is the average distance needed to move the probability mass of one distribution to morph into the other. For the normal distributions z_1 and z_2 , the Wasserstein-2 distance is defined as

$$W(z_1, z_2) = \sqrt{(\mu_1 - \mu_2)^2 + (\sigma_1 - \sigma_2)^2}. \quad (12)$$

The distances in Eq. (11) and Eq. (12) will be used in the acquisition functions presented in Sec. 4.

3. Methodology

We now present our main contributions. In Sec. 3.1, we introduce SAL, a novel family of metrics for Bayesian active learning. In Sec. 3.2, we extend this to SCoreBO, the first acquisition function for joint Bayesian optimization and active learning of hyperparameters, inspired by information-theoretic Bayesian optimization acquisition functions. In Sec. 3.3, we demonstrate how to efficiently approximate multiple types of statistical distances.

3.1. Statistical distance-based Active Learning

In active learning for GPs, it is important to efficiently learn the correct model hyperparameters. By measuring where the posterior hyperparameter uncertainty causes high disagreement in model output, the search can be focused on where the hyperparameter uncertainty has a high impact. However, considering only the posterior disagreement in mean, as in BQBC, is overly restrictive and does not fully utilize the available distributions for the hyperparameters. For example, it ignores uncertainty in the outputscale hyperparameter of the Gaussian process, which disincentivizes exploration. As such, we propose to generalize the acquisition function in Eq. (8) to instead consider the posterior disagreement as measured by any metric that acts on statistical distributions. Intuitively, locations where the posterior distribution changes significantly as a result of model uncertainty will qualify as good points to sample to quickly learn the model hyperparameters. When an observation at such a location is obtained, hyperparameters which yielded an incorrect model prediction at the location will have a substantially smaller likelihood, which in turn aids hyperparameter convergence. In Eq. (13), the SAL acquisition function is displayed,

$$\alpha_{SAL}(\mathbf{x}) = \mathbb{E}_{\boldsymbol{\theta}}[d(p(y_{\mathbf{x}}|\boldsymbol{\theta}, \mathcal{D}), p(y_{\mathbf{x}}|\mathcal{D}))] \quad (13)$$

$$\approx \frac{1}{M} \sum_{m=1}^M d(p(y_{\mathbf{x}}|\boldsymbol{\theta}_m, \mathcal{D}), p(y_{\mathbf{x}}|\mathcal{D})) \quad (14)$$

where M is the number of hyperparameter samples drawn from its associated posterior, $\boldsymbol{\theta}_m \sim p(\boldsymbol{\theta}|\mathcal{D})$, $\boldsymbol{\theta} = \{\ell, \sigma_f, \sigma_\varepsilon\}$, and d is a statistical distance metric.

In Fig. 2, the SAL acquisition function is visualized. The marginal posterior (left) is made up of three vastly different conditional posteriors - one with high outputscale (blue), one with very high noise (orange), and one with small outputscale (green). For each of the blue, orange and green conditionals, the distance to the marginal posterior is computed. Intuitively, disagreement in noise level σ_ε can cause large posterior disagreement at already queried locations. Similarly, uncertainty in outputscale σ_f between posteriors will yield disagreement in large-variance regions, which will result in global variance reduction. Compared to other active learning acquisition functions, SAL carries distinct advantages: it has incentive to query the same location multiple times to quickly estimate noise levels, and accomplishes the typical active learning objectives of predictive accuracy and global exploration by alleviating uncertainty over the lengthscales and outputscale of the GP.

3.2. Self-Correcting Bayesian Optimization (SCoreBO)

Equipped with the active learning objective from Eq. (13), we have an intuitive measure for the hyperparameter-induced posterior disagreement, which incentivizes hyperparameter learning by querying locations where disagreement is the largest. As we show in our experiments (Sec. 4.1), the acquisition function in Eq. (13) performs well for active learning tasks and reduces hyperparameter uncertainty at improved rates. However, it does not inherently carry an incentive to optimize the function at hand. To inject an optimization objective into Eq. (13), we draw inspiration from information-theoretic BO and further condition on samples of the optimum which yields an additional source of disagreement reserved for promising regions of the search space.

We consider (\mathbf{x}^*, f^*) , representing the global optimal optimum and optimal value considered in the JES acquisition function (Hvarfner et al., 2022a; Tu et al., 2022), as hyperparameters. When conditioning on (\mathbf{x}^*, f^*) , we condition on an additional (optimal) observation, and the posterior over f becomes an upper truncated Gaussian, reducing the variance and pushing the mean marginally downwards in uncertain regions far away from the optimum as visualized in Fig. 3. As such, sampling and conditioning on (\mathbf{x}^*, f^*) introduces an additional source of disagreement between

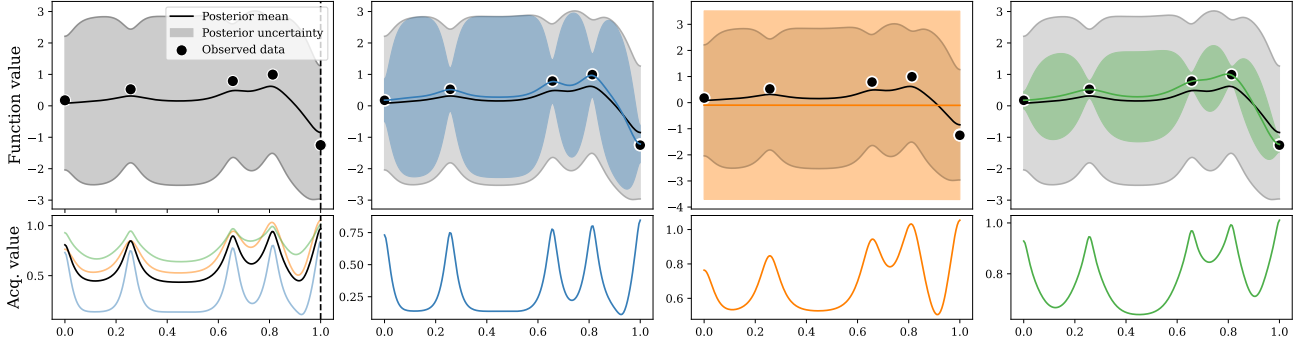


Figure 2. Marginal posterior (top left), α_{SAL} using the Wasserstein distance (top left, grey), and the three conditional GPs (blue, orange, green) and their marginal contribution to the total acquisition function (bottom row). The large disagreement in noise level and lengthscale, primarily caused by the orange GP (large noise, long lengthscale), makes α_{SAL} query the lowest-valued point for a second time (selected location as vertical dashed line in the leftmost plot) to determine the mean and variance at that location.

the marginal posterior and the conditionals. The higher the probability density $f(x) > f^*$ under the unconditioned GP, the more the distribution is skewed. The optimizer (x^*, f^*) is obtained through posterior sampling (Wilson et al., 2020) and gradient-based optimization of the samples.

Utilizing the lower bound on the change in the posterior induced by conditioning on (x^*, f^*) , as derived in GIBBON (Moss et al., 2021), we approximate the posterior $p(y_x|\theta, x^*, f^*, \mathcal{D})$ conditioned on both hyperparameters θ and optimizer (x^*, f^*) , with a Gaussian distribution $\hat{p}(y_x|\theta, f^*, \mathcal{D})$ by moment matching the two first moments to the true posterior, which is an extended skew distribution (Nguyen et al., 2022). Denoting (x^*, f^*) as $*$, the SCoreBO acquisition function becomes

$$\alpha_{SC}(x) = \mathbb{E}_{\theta, *}[d(p(y_x|\mathcal{D}), p(y_x|\theta, *, \mathcal{D}))]. \quad (15)$$

The joint posterior $p(\theta, *|\mathcal{D}) = p(*|\theta, \mathcal{D})p(\theta|\mathcal{D})$ used for the expectation in Eq. (15) can be achieved by hierarchical sampling. We first draw hyperparameters θ and thereafter optimizers $*|\theta$. As such, the expression for the SCoreBO acquisition function is:

$$\alpha(x) \approx \frac{1}{NM} \sum_{m=1}^M \sum_{n=1}^N d(p(y_x|\mathcal{D}), p(y_x|\theta_m, *_{\theta_m, n}|\mathcal{D})), \quad (16)$$

where N is the number of optimizers sampled per hyperparameter set. Notably, while the acquisition function in (15) considers the optimizer (x^*, f^*) , similarly to JES, SCoreBO is not restricted to employing that quantity alone. Drawing parallels to PES and MES, we can also choose to condition on either x^* or f^* alone in place of (x^*, f^*) . Choosing to do so introduces a smaller disagreement in the posterior at the conditioned location x^* , thus decreasing the acquisition value there. This will in turn decrease the emphasis that SCoreBO puts on optimization, relative to hyperparameter learning. In Fig. 3, the SCoreBO acquisi-

Algorithm 1 SCoreBO iteration

- 1: **Input:** Number of hyperparameter sets M , number of sampled optima N , current data \mathcal{D}
- 2: **Output:** Next query location x' .
- 3: **for** $m \in \{1, \dots, M\}$ **do**
- 4: $\theta_m \sim p(\theta|\mathcal{D})$
- 5: **for** $n \in \{1, \dots, N\}$ **do**
- 6: $*_{\theta_m, n} \leftarrow \max f_{\theta_m, n}, f_{\theta_m, n} \sim p(f|\theta_m)$
- 7: $p(y_x|\theta_m, *_{\theta_m, n}) \leftarrow \text{CondGP}(*_{\theta_m, n}, \theta_m, \mathcal{D})$
- 8: **end for**
- 9: **end for**
- 10: $x' = \arg \max \alpha(x)$ {defined in Eq. (16)}

tion function is displayed for the same situation as in Fig. 2. By conditioning on $M = 2$ optimizers per GP (displaying the resulting GP for one of them), the mean is pushed upwards around the extra observation and the posterior predictive distribution over f is truncated as it is now upper bounded by f^* . While the location that was most attractive under the active learning objective is still attractive, the best location to query is now a point that is more likely to be optimal, but still attractive under the original active learning objective.

Alg. 1 displays how the involved densities are formed for one iteration of SCoreBO. For each hyperparameter set, a number of optima are sampled and individually conditioned on (CondGP) given the current data and hyperparameter set. After this procedure is completed for all hyperparameter sets, the statistical distance between each conditional posterior and the marginal is computed.

3.3. Approximation of Statistical Distances

We consider two proper statistical distances, Wasserstein distance and Hellinger distance, where the former is used for SAL and the latter for SCoreBO. In contrast to BQBC,

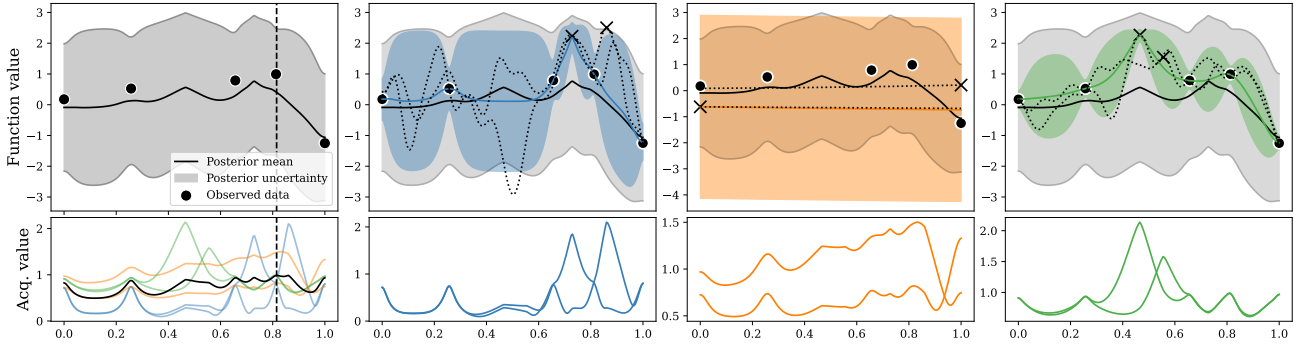


Figure 3. Approximate marginal posterior after having conditioned on (\mathbf{x}^*, f^*) (top left), α_{SC} using the Wasserstein distance (bottom left), the three conditional truncated posteriors and their marginal contribution to the total acquisition function for the same iteration as Fig. 2. Conditioning on (\mathbf{x}^*, f^*) (marked as \times) pushes the posterior downwards, introducing additional disagreement between the marginal posterior and the sampled GPs in promising regions as a result of conditioning. In the figure, we marginalize over $M = 3$ sets of hyperparameters and $N = 2$ optimizers per GP, where each optimizer’s contribution to the acquisition function is visible under its corresponding GP.

the statistical distance between the normally distributed conditionals and the marginal posterior predictive distribution, which is a Gaussian mixture, is not generally available in closed-form. We propose two approaches: estimating the distances using sampling, which is more expensive but asymptotically unbiased, and estimation using moment matching, which emphasizes practicality and simplicity.

Approximation through sampling Using Monte Carlo, different distances are most efficiently estimated in different manners. To compute the Wasserstein distance, we utilize quasi-Monte Carlo. From the definition of the distance in one dimension, we obtain

$$W^2(p, q) = \int_0^1 |Q(u) - P(u)|^2 du \approx \sum_{\ell=1}^L |Q(u_\ell) - P(u_\ell)|^2, \tag{17}$$

where $u_\ell \sim \mathcal{U}(0, 1)$, and $P(x)$ and $Q(x)$ are the respective cumulative distributions for $p(x)$ and $q(x)$.

To compute the Hellinger distance, we obtain

$$H^2(p, q) = 1 - \int_{\mathcal{X}} \sqrt{\frac{q(x)}{p(x)}} p(x) dx \approx 1 - \sum_{\ell=1}^L \sqrt{\frac{q(x_\ell)}{p(x_\ell)}}, \tag{18}$$

where $x_\ell \sim p(x)$ is sampled using MC. In ScoreBO, $p(x)$ is the marginal $p(y_{\mathbf{x}}|\mathcal{D})$, and $q(x)$ each of the various conditionals $p(y_{\mathbf{x}}|\ast, \theta, \mathcal{D})$.

Moment Matching of Marginal Posterior Secondly, we propose to fully utilize the closed-form expressions of the involved distances for Gaussians, and approximate the full posterior mixture $p(y_{\mathbf{x}}|\mathcal{D})$ with a Gaussian distribution using moment matching (MM) for the first and second moment. While a Gaussian mixture is not generally well approximated by a Normal distribution, we show empirically

in App. D that the distance between the conditionals and the approximate posterior is. Moment matching circumvents a quadratic cost $\mathcal{O}(N^2M^2)$ in the number of samples of each pass through the acquisition function, and yields comparable performance to the estimation procedures proposed above. In App. D, we qualitatively assess the accuracy of the MM approach for both distances, and display its ability to preserve the shape of the acquisition function.

4. Experiments

In this section we showcase the performance of the SAL and ScoreBO acquisition functions on a variety of tasks. For active learning, SAL shows state-of-the-art performance on a majority of benchmarks, and yields more reliably good results than any of the baselines. For the optimization tasks, ScoreBO more efficiently learns the model hyperparameters, and outperforms prominent Bayesian optimization acquisition functions on a variety of tasks. All experiments are implemented in BOTorch (Balandat et al., 2020)¹. We use the same priors for the model hyperparameters as Riis et al. (2022) for ease of comparison, which is a log-normal distribution $\mathcal{LN}(0, 3)$ for all hyperparameters. The complete experimental setup is presented in detail in Appendix A, and our code is publicly available at <https://github.com/scorebo/scorebo.git>.

For the active learning experiments, we use the Wasserstein distance, and for the BO experiments, we use the Hellinger distance. These two distance measures were observed to be the most and least explorative of the search space among the ones tested. The Hellinger distance of ScoreBO was generally well calibrated for BO, whereas the Wasserstein distance was deemed too exploratory. This trait, however,

¹<https://botorch.org/>

made the Wasserstein distance a great candidate for active learning. We display the active learning performance of all the tested distance measures in App. B.2. Moreover, we display the performance of both the Hellinger and Wasserstein variant of ScoreBO in Fig. 13.

4.1. Active Learning Tasks

To evaluate the performance of our statistical distance-based active learning acquisition function, we compare it with the 3 baseline methods BALM, BOBC and QBMGP on the same six functions used by Riis et al. (2022). The benchmarks are chosen for their irregular shape: Gramacy1D has a subtle periodicity that is hard to distinguish from noise, Higdon and Gramacy2D varies significantly in characteristics in different regions, and Branin, Hartmann-6 and Ishigami have a generally nonlinear structure. We use the Wasserstein distance, denoted as SAL-WS.

To compare the different baselines we compare their predictive power measured by the Root Mean Square Error (RMSE) of the model predictions over a large set of validation points. In Fig. 4, we show how the RMSE changes with increasing training data. SAL-WS shows consistent top performance. Overall, SAL-WS and BOBC perform best, outperforming the other baselines by a substantial margin on half of all tasks. SAL-WS is, however, better on Gramacy-1D and Gramacy-2D, and consistently among the best methods. Both BALM and QBMGP stagnate early on Hartmann-6, and perform subpar for a long time on Ishigami. In App. B.2, Fig. 10, we show the evolution of the average marginal log likelihood (MLL) of the same set of validation points. MLL emphasizes appropriate predictive uncertainty in addition to accurate predictive mean. SAL-WS performs similarly well on this metric, which further emphasizes its ability to accurately model the function at hand. In App. B.2, Fig. 14, we display the ability of the various acquisition functions to learn the hyperparameters of the model. In particular, SAL-HR prioritizes hyperparameter learning at the expense of predictive accuracy.

4.2. Bayesian Optimization Tasks

For the Bayesian optimization tasks, we consider the joint conditioning (JES-like) variant of ScoreBO, i.e., conditioning on (x^*, f^*) . We benchmark against a number of state-of-the-art baselines from the BO literature: EI for noisy experiments (Bull, 2011; Jones et al., 1998; Letham et al., 2018), as well as JES (Hvarfner et al., 2022a; Tu et al., 2022) and the MES approach GIBBON (Moss et al., 2021; Wang & Jegelka, 2017).

Efficiently learning the hyperparameters To showcase ScoreBO’s ability to find the correct model hyperparameters, we run all relevant acquisition functions on samples

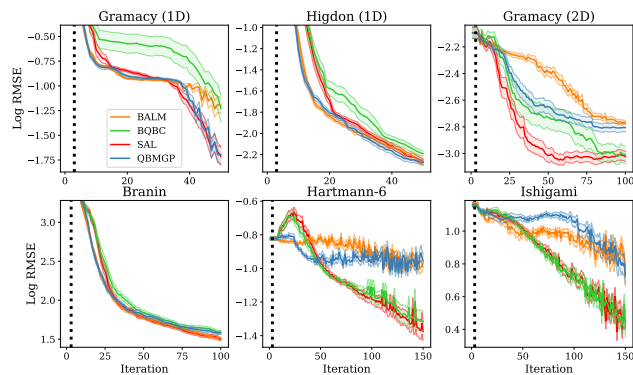


Figure 4. Log RMSE on six active learning functions for BALM, BOBC, QBMGP and SAL using Wasserstein distance. We plot mean and one standard error for 25 repetitions.

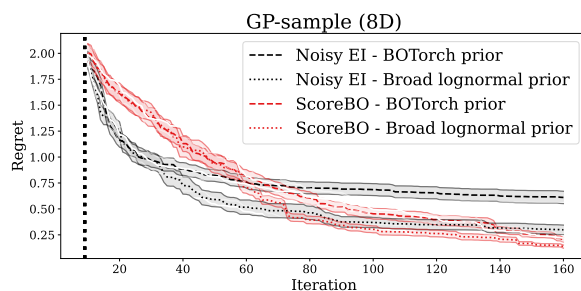


Figure 5. Regret for EI and ScoreBO on the 8-dimensional GP sample for two different types of hyperparameter priors. Mean and standard deviation are plotted for all hyperparameter samples across 20 repetitions.

from the 8-dimensional GP in Fig. 1. We exploit that for GP samples, the objectively true hyperparameters are known as ground truth (in contrast to typical synthetic test functions). We utilize the same priors as in Fig. 1 on all the hyperparameters and compare ScoreBO to EI to assess the ability of each acquisition function to work independently of the choice of starting hyperparameters. In Fig. 5, for each acquisition function, we plot the log regret across 20 different 8-dimensional instances of this task. The tasks at hand have lengthscales that vary substantially between dimensions, with one dimension of very short lengthscale, two dimensions of short lengthscales, two of moderate lengthscales, and three dimensions that are effectively unimportant. As such, identifying dimensions of substantial importance is crucial to optimizing the functions.

The explanation for this good performance can be seen in Fig. 15 in App. C. Here, we show how the mean and uncertainty of each hyperparameter evolve over time, with the dashed line marking the true of each. We note that the hyperparameters of ScoreBO converge faster towards the correct values than those of EI, both in terms of accuracy of the mean and the uncertainty, for all lengthscales and the

outputscale. EI, however, is slightly more accurate in the estimation of the noise variance, which can be explained by its well-documented (Qin et al., 2017) greedy behavior. Sampling points in very close vicinity to each other is efficient for estimating the noise. In App. C, we display the hyperparameter convergence of SCoreBO and EI for both types of priors.

Synthetic test functions We run SCoreBO on a number of synthetic test functions commonly used for BO, and present how the log inference regret evolves over the iterations in Fig. 6. All benchmarks are perturbed by Gaussian noise. We evaluate inference regret, i.e., the current best guess of the optimal location $\arg \max_{\mathbf{x}} \bar{\mu}(\mathbf{x})$, which is conventional for non-myopic acquisition functions (Hennig & Schuler, 2012a; Hernández-Lobato et al., 2014; Hvarfner et al., 2022a). SCoreBO yields the best inference regret on four of the six tasks.

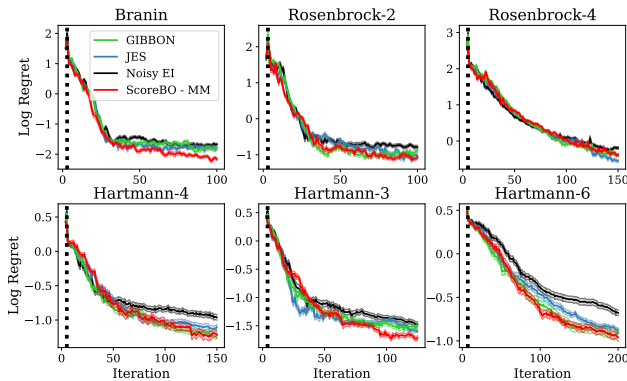


Figure 6. Average log inference regret for SCoreBO, JES, GIBBON and noisy EI on six synthetic test functions.

4.3. A Practical Need for Self-correction

Lastly, we evaluate the performance of SCoreBO on tasks which emphasize model correctness to a large degree. Such tasks involve exotic assumptions on the model, and provide enhanced optimization if satisfied. We focus on two domains: (1) high-dimensional Bayesian optimization through sparse adaptive axis-aligned priors (SAASBO) (Eriksson & Jankowiak, 2021) and (2) Bayesian optimization with additively decomposable structure (Gardner et al., 2017; Kandasamy et al., 2015). Eriksson & Jankowiak (2021) consider their proposed method for noiseless tasks, where active variables easily distinguish from their non-active counterparts. However, SAASBO is not inherently restricted to noiseless problems. A similar argument can be made for (Gardner et al., 2017), where parameter cross-covariances (and the lack thereof) are substantially more difficult to identify in the presence of noise.

In Fig. 7, we visualize the performance of SCoreBO with

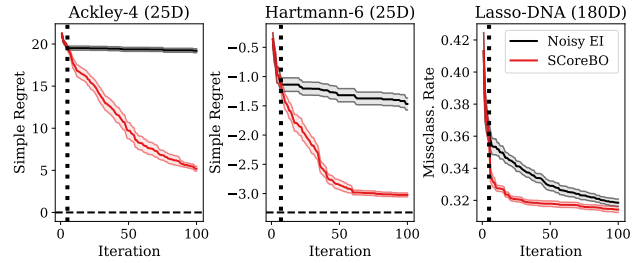


Figure 7. Final loss using SAASBO priors on the noisy embedded Ackley-4, embedded Hartmann-6 and the DNA classification task, mean and one standard error. SCoreBO identifies the important dimensions rapidly, and successfully optimizes the tasks.

SAASBO priors on two noisy benchmarks, Ackley-4 and Hartmann-6, with dummy dimensions added as well as a real-world benchmark where a weighted Lasso model in 180 dimensions is fitted (Šehić et al., 2021). We compare it to NoisyEI, also with SAASBO priors. In such benchmarks, where finding the correct hyperparameters is of additional importance, we see that SCoreBO easily outperforms traditional methods. To further exemplify how SCoreBO identifies the relevant dimensions, in Fig. 8, we show how the hyperparameters evolve on the Ackley-4 task. SCoreBO quickly finds the correct lengthscales and outputscale with high certainty ($l_1, \dots, l_4 \approx 10^{-1}$, $l_5, \dots, l_{25} \approx 10^1$), whereas EI remains uncertain of which dimensions are active throughout the optimization procedure.

Lastly, we demonstrate the ability of SCoreBO to self-correct on kernel uncertainty, by considering tasks with additive decompositions. We utilize the approach of (Gardner et al., 2017), where additive decompositions are marginalized over. Ideally, a sufficiently accurate decomposition is found quickly, which rapidly speeds up optimization. In Fig. 9, we demonstrate on two GP sample tasks (left, middle) and demonstrate the ability of SCoreBO to find the correct additive decompositions (right). We observe that SCoreBO makes substantially fewer incorrect splits at earlier iterations than EI, and rarely proposes any incorrect splits at later iterations.

5. Conclusion and Future Work

The Gaussian process hyperparameters play an integral role in the efficiency of both Bayesian optimization and active learning applications. In this paper, we propose Statistical distance-based Active Learning (SAL) and Self-Correcting Bayesian Optimization (SCoreBO), two acquisition functions that explicitly consider hyperparameter-induced disagreement in the posterior distribution when selecting which points to query. By doing so, we achieve high-end performance on both active learning and Bayesian optimization tasks, and successfully learn hyperparameters at improved rates compared to conventional Bayesian optimization. SAL

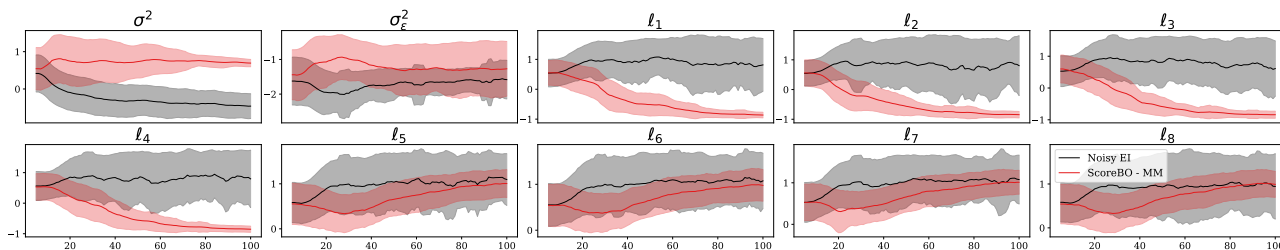


Figure 8. Hyperparameter convergence on the 25-D-embedded 4D Ackley function with a SAASBO HP prior. Log HP mean and 1 standard deviation is plotted per iteration. SCoreBO identifies ℓ_1, \dots, ℓ_4 as important (short lengthscales) with low uncertainty. Moreover, ℓ_5, \dots, ℓ_8 are correctly identified as dummy dimensions. EI fails to identify any important lengthscales.

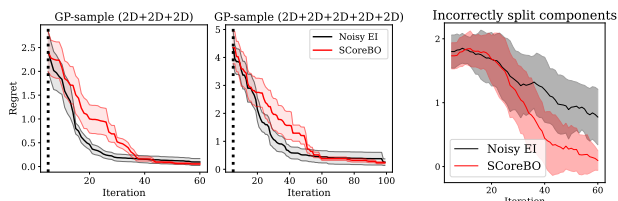


Figure 9. Final value of using AddGPs on 6D and 10D GP sample functions, fully decomposable in groups of two. SCoreBO achieves better final performance (left, middle) with low uncertainty, and successfully finds the additive components of the 6D task (right).

and SCoreBO establishes a new performance baseline for both active learning and Bayesian optimization tasks, and breaks ground for new methods in the space of joint active learning and optimization of black-box functions.

For future work, we will investigate further how SAL’s efficiency is affected by the choice of distance metric, and how various distance metrics emphasize different aspects of learning. In BO, SCoreBO can allow for increased model complexity in BO applications. Moreover, global trends, such as non-constant means (De Ath et al., 2020), is yet another avenue in which SCoreBO can accelerate learning. All of these approaches potentially stand to benefit from the joint AL-BO framework that SCoreBO provides.

Acknowledgements

Luigi Nardi was supported in part by affiliate members and other supporters of the Stanford DAWN project — Ant Financial, Facebook, Google, Intel, Microsoft, NEC, SAP, Teradata, and VMware. Carl Hvarfner and Luigi Nardi were partially supported by the Wallenberg AI, Autonomous Systems and Software Program (WASP) funded by the Knut and Alice Wallenberg Foundation. Luigi Nardi was partially supported by the Wallenberg Launch Pad (WALP) grant Dnr 2021.0348. Frank Hutter acknowledges support through TAILOR, a project funded by the EU Horizon 2020 research and innovation programme under GA No 952215, by the Deutsche Forschungsgemeinschaft (DFG, German

Research Foundation) under grant number 417962828, by the state of Baden-Württemberg through bwHPC and the German Research Foundation (DFG) through grant no INST 39/963-1 FUGG, and by the European Research Council (ERC) Consolidator Grant “Deep Learning 2.0” (grant no. 101045765). The computations were also enabled by resources provided by the Swedish National Infrastructure for Computing (SNIC) at LUNARC partially funded by the Swedish Research Council through grant agreement no. 2018-05973. Funded by the European Union. Views and opinions expressed are however those of the author(s) only and do not necessarily reflect those of the European Union or the ERC. Neither the European Union nor the ERC can be held responsible for them.



Funded by
the European Union

References

- Balandat, M., Karrer, B., Jiang, D. R., Daulton, S., Letham, B., Wilson, A. G., and Bakshy, E. Botorch: A framework for efficient monte-carlo bayesian optimization. In *Advances in Neural Information Processing Systems*, 2020. URL <http://arxiv.org/abs/1910.06403>.
- Berkenkamp, F., Krause, A., and Schoellig, A. Bayesian optimization with safety constraints: Safe and automatic parameter tuning in robotics. *Machine Learning*, 06 2021. doi: 10.1007/s10994-021-06019-1.
- Bingham, E., Chen, J. P., Jankowiak, M., Obermeyer, F., Pradhan, N., Karaletsos, T., Singh, R., Szerlip, P., Horsfall, P., and Goodman, N. D. Pyro: Deep Universal Probabilistic Programming. *Journal of Machine Learning Research*, 2018.
- Binois, M., Huang, J., Gramacy, R. B., and Ludkovski, M. Replication or exploration? sequential design for stochastic simulation experiments. *Technometrics*, 61(1): 7–23, 2019.

- Bull, A. D. Convergence rates of efficient global optimization algorithms. 12:2879–2904, 2011.
- Calandra, R., Gopalan, N., Seyfarth, A., Peters, J., and Deisenroth, M. Bayesian gait optimization for bipedal locomotion. In Pardalos, P. and Resende, M. (eds.), *Proceedings of the Eighth International Conference on Learning and Intelligent Optimization (LION'14)*, 2014.
- Chen, Y., Huang, A., Wang, Z., Antonoglou, I., Schrittwieser, J., Silver, D., and de Freitas, N. Bayesian optimization in alphago. *CoRR*, abs/1812.06855, 2018. URL <http://arxiv.org/abs/1812.06855>.
- Cohn, D. A. Neural network exploration using optimal experiment design. *Neural networks*, 9(6):1071–1083, 1996.
- Cowen-Rivers, A. I., Lyu, W., Wang, Z., Tutunov, R., Hao, J., Wang, J., and Bou-Ammar, H. HEBO: heteroscedastic evolutionary bayesian optimisation. *CoRR*, abs/2012.03826, 2020. URL <https://arxiv.org/abs/2012.03826>.
- De Ath, G., Fieldsend, J. E., and Everson, R. M. What do you mean? the role of the mean function in bayesian optimisation. In *Proceedings of the 2020 Genetic and Evolutionary Computation Conference Companion, GECCO '20*, pp. 1623–1631, New York, NY, USA, 2020. Association for Computing Machinery. ISBN 9781450371278. doi: 10.1145/3377929.3398118. URL <https://doi.org/10.1145/3377929.3398118>.
- Ejjeh, A., Medvinsky, L., Councilman, A., Nehra, H., Sharma, S., Adve, V., Nardi, L., Nurvitadhi, E., and Rutenbar, R. A. Hpv2fpga: Enabling true hardware-agnostic fpga programming. In *Proceedings of the 33rd IEEE International Conference on Application-specific Systems, Architectures, and Processors*, 2022.
- Eriksson, D. and Jankowiak, M. High-dimensional Bayesian optimization with sparse axis-aligned subspaces. In de Campos, C. and Maathuis, M. H. (eds.), *Proceedings of the Thirty-Seventh Conference on Uncertainty in Artificial Intelligence*, volume 161 of *Proceedings of Machine Learning Research*, pp. 493–503. PMLR, 27–30 Jul 2021. URL <https://proceedings.mlr.press/v161/eriksson21a.html>.
- Eriksson, D., Pearce, M., Gardner, J., Turner, R. D., and Poloczek, M. Scalable global optimization via local bayesian optimization. In Wallach, H., Larochelle, H., Beygelzimer, A., d'Alché-Buc, F., Fox, E., and Garnett, R. (eds.), *Advances in Neural Information Processing Systems*, volume 32. Curran Associates, Inc., 2019. URL <https://proceedings.neurips.cc/paper/2019/file/6c990b7aca7bc7058f5e98ea909e924b-Paper.pdf>.
- Frazier, P. I. A tutorial on bayesian optimization. *arXiv preprint arXiv:1807.02811*, 2018.
- Frazier, P. I. and Wang, J. Bayesian optimization for materials design. In *Information science for materials discovery and design*, pp. 45–75. Springer, 2016.
- Gardner, J., Guo, C., Weinberger, K., Garnett, R., and Grosse, R. Discovering and Exploiting Additive Structure for Bayesian Optimization. In Singh, A. and Zhu, J. (eds.), *Proceedings of the Seventeenth International Conference on Artificial Intelligence and Statistics (AISTATS)*, volume 54, pp. 1311–1319. Proceedings of Machine Learning Research, 2017.
- Griffiths, R.-R. and Hernández-Lobato, J. M. Constrained bayesian optimization for automatic chemical design. *arXiv: Machine Learning*, 2017.
- Hennig, P. and Schuler, C. Entropy search for information-efficient global optimization. 98888(1):1809–1837, 2012a.
- Hennig, P. and Schuler, C. J. Entropy search for information-efficient global optimization. *Journal of Machine Learning Research*, 13(1):1809–1837, June 2012b. ISSN 1532-4435.
- Hernández-Lobato, J. M., Hoffman, M. W., and Ghahramani, Z. Predictive entropy search for efficient global optimization of black-box functions. In *Advances in Neural Information Processing Systems*, 2014. URL <https://proceedings.neurips.cc/paper/2014/file/069d3bb002acd8d7dd095917f9efe4cb-Paper.pdf>.
- Hoffman, M. D. and Gelman, A. The no-u-turn sampler: Adaptively setting path lengths in hamiltonian monte carlo. *Journal of Machine Learning Research*, 15(47):1593–1623, 2014. URL <http://jmlr.org/papers/v15/hoffman14a.html>.
- Houlsby, N., Huszár, F., Ghahramani, Z., and Lengyel, M. Bayesian active learning for classification and preference learning. *arXiv preprint arXiv:1112.5745*, 2011.
- Hutter, F., Hoos, H., and Leyton-Brown, K. Sequential model-based optimization for general algorithm configuration. In Coello, C. (ed.), *Proceedings of the Fifth International Conference on Learning and Intelligent Optimization (LION'11)*, volume 6683, pp. 507–523, 2011.
- Hutter, F., Lindauer, M., Balint, A., Bayless, S., Hoos, H., and Leyton-Brown, K. The configurable SAT solver challenge (CSSC). 243:1–25, 2017.

- Hvarfner, C., Hutter, F., and Nardi, L. Joint entropy search for maximally-informed bayesian optimization. *arXiv preprint arXiv:2206.04771*, 2022a.
- Hvarfner, C., Stoll, D., Souza, A., Nardi, L., Lindauer, M., and Hutter, F. PiBO: Augmenting Acquisition Functions with User Beliefs for Bayesian Optimization. In *International Conference on Learning Representations*, 2022b.
- Jones, D., Schonlau, M., and Welch, W. Efficient global optimization of expensive black box functions. 13:455–492, 1998.
- Kandasamy, K., Schneider, J., and Póczos, B. High Dimensional Bayesian Optimisation and Bandits via Additive Models. In Bach, F. and Blei, D. (eds.), *Proceedings of the 32nd International Conference on Machine Learning (ICML’15)*, volume 37, pp. 295–304. Omnipress, 2015.
- Kandasamy, K., Neiswanger, W., Schneider, J., Poczos, B., and Xing, E. P. Neural architecture search with bayesian optimisation and optimal transport. *Advances in neural information processing systems*, 31, 2018.
- Kirsch, A., Van Amersfoort, J., and Gal, Y. Batchbald: Efficient and diverse batch acquisition for deep bayesian active learning. *Advances in neural information processing systems*, 32, 2019.
- Lalchand, V. and Rasmussen, C. E. Approximate inference for fully bayesian gaussian process regression. In *Symposium on Advances in Approximate Bayesian Inference*, pp. 1–12. PMLR, 2020.
- Letham, B., Brian, K., Ottoni, G., and Bakshy, E. Constrained Bayesian optimization with noisy experiments. *Bayesian Analysis*, 2018.
- MacKay, D. and Neal, R. Automatic relevance detection for neural networks. Technical report, University of Cambridge, 1994.
- MacKay, D. J. Information-based objective functions for active data selection. *Neural computation*, 4(4):590–604, 1992.
- Malkomes, G., Schaff, C., and Garnett, R. Bayesian optimization for automated model selection. In Hutter, F., Kotthoff, L., and Vanschoren, J. (eds.), *Proceedings of the Workshop on Automatic Machine Learning*, volume 64 of *Proceedings of Machine Learning Research*, pp. 41–47, New York, New York, USA, 24 Jun 2016. PMLR. URL https://proceedings.mlr.press/v64/malkomes_bayesian_2016.html.
- Mayr, M., Ahmad, F., Chatzilygeroudis, K. I., Nardi, L., and Krüger, V. Skill-based Multi-objective Reinforcement Learning of Industrial Robot Tasks with Planning and Knowledge Integration. *CoRR*, abs/2203.10033, 2022a. URL <https://doi.org/10.48550/arXiv.2203.10033>.
- Mayr, M., Hvarfner, C., Chatzilygeroudis, K., Nardi, L., and Krueger, V. Learning skill-based industrial robot tasks with user priors. *IEEE 18th International Conference on Automation Science and Engineering*, 2022b. URL <https://arxiv.org/abs/2208.01605>.
- Moss, H. B., Leslie, D. S., Gonzalez, J., and Rayson, P. Gibbon: General-purpose information-based bayesian optimisation. *Journal of Machine Learning Research*, 22(235):1–49, 2021. URL <http://jmlr.org/papers/v22/21-0120.html>.
- Nardi, L., Koeplinger, D., and Olukotun, K. Practical design space exploration. In *2019 IEEE 27th International Symposium on Modeling, Analysis, and Simulation of Computer and Telecommunication Systems (MASCOTS)*, pp. 347–358. IEEE, 2019.
- Nguyen, Q. P., Low, B. K. H., and Jaillet, P. Rectified max-value entropy search for bayesian optimization, 2022. URL <https://arxiv.org/abs/2202.13597>.
- Osborne, M. A. *Bayesian Gaussian processes for sequential prediction, optimisation and quadrature*. PhD thesis, Oxford University, UK, 2010.
- Papenmeier, L., Nardi, L., and Poloczek, M. Increasing the scope as you learn: Adaptive bayesian optimization in nested subspaces. In Oh, A. H., Agarwal, A., Belgrave, D., and Cho, K. (eds.), *Advances in Neural Information Processing Systems*, 2022. URL <https://openreview.net/forum?id=e4Wf6112DI>.
- Qin, C., Klabjan, D., and Russo, D. Improving the expected improvement algorithm. In *Proceedings of the 31st International Conference on Neural Information Processing Systems, NIPS’17*, pp. 5387–5397, Red Hook, NY, USA, 2017. Curran Associates Inc. ISBN 9781510860964.
- Rasmussen, C. and Williams, C. *Gaussian Processes for Machine Learning*. The MIT Press, 2006.
- Riis, C., Antunes, F. N., Hüttel, F. B., Azevedo, C. L., and Pereira, F. C. Bayesian active learning with fully bayesian gaussian processes. *arXiv preprint arXiv:2205.10186*, 2022.
- Ru, B., Osborne, M. A., Mcleod, M., and Granzol, D. Fast information-theoretic Bayesian optimisation. In Dy, J. and Krause, A. (eds.), *Proceedings of the 35th International Conference on Machine Learning*, volume 80 of *Proceedings of Machine Learning Research*, pp. 4384–4392. PMLR, 10–15 Jul 2018. URL <https://proceedings.mlr.press/v80/ru18a.html>.

- Ru, B., Wan, X., Dong, X., and Osborne, M. Interpretable neural architecture search via bayesian optimization with weisfeiler-lehman kernels. *arXiv preprint arXiv:2006.07556*, 2020.
- Šehić, K., Gramfort, A., Salmon, J., and Nardi, L. LasoBench: A High-Dimensional Hyperparameter Optimization Benchmark Suite for Lasso. *arXiv preprint arXiv:2111.02790*, 2021.
- Settles, B. Active learning literature survey. 2009.
- Snoek, J., Larochelle, H., and Adams, R. Practical Bayesian optimization of machine learning algorithms. In Bartlett, P., Pereira, F., Burges, C., Bottou, L., and Weinberger, K. (eds.), *Proceedings of the 26th International Conference on Advances in Neural Information Processing Systems (NeurIPS'12)*, pp. 2960–2968, 2012.
- Snoek, J., Swersky, K., Zemel, R., and Adams, R. Input warping for Bayesian optimization of non-stationary functions. In Xing, E. and Jebara, T. (eds.), *Proceedings of the 31th International Conference on Machine Learning (ICML'14)*, pp. 1674–1682. Omnipress, 2014.
- Srinivas, N., Krause, A., Kakade, S. M., and Seeger, M. W. Information-theoretic regret bounds for gaussian process optimization in the bandit setting. *IEEE Transactions on Information Theory*, 58(5):3250–3265, May 2012. ISSN 1557-9654. doi: 10.1109/tit.2011.2182033. URL <http://dx.doi.org/10.1109/TIT.2011.2182033>.
- Takeno, S., Fukuoka, H., Tsukada, Y., Koyama, T., Shiga, M., Takeuchi, I., and Karasuyama, M. Multi-fidelity Bayesian optimization with max-value entropy search and its parallelization. In III, H. D. and Singh, A. (eds.), *Proceedings of the 37th International Conference on Machine Learning*, volume 119 of *Proceedings of Machine Learning Research*, pp. 9334–9345. PMLR, 13–18 Jul 2020. URL <https://proceedings.mlr.press/v119/takeno20a.html>.
- Tu, B., Gandy, A., Kantas, N., and Shafei, B. Joint entropy search for multi-objective bayesian optimization. In Oh, A. H., Agarwal, A., Belgrave, D., and Cho, K. (eds.), *Advances in Neural Information Processing Systems*, 2022. URL <https://openreview.net/forum?id=ZChgD8OoGds>.
- Wan, X., Nguyen, V., Ha, H., Ru, B., Lu, C., and Osborne, M. A. Think global and act local: Bayesian optimisation over high-dimensional categorical and mixed search spaces. *International Conference on Machine Learning (ICML) 38*, 2021.
- Wang, Z. and Jegelka, S. Max-value entropy search for efficient bayesian optimization. In *International Conference on Machine Learning (ICML)*, 2017.
- Wilson, J. T., Borovitskiy, V., Terenin, A., Mostowsky, P., and Deisenroth, M. P. Efficiently sampling functions from gaussian process posteriors. In *International Conference on Machine Learning*, 2020. URL <https://arxiv.org/abs/2002.09309>.
- Yao, Y., Vehtari, A., and Gelman, A. Stacking for non-mixing bayesian computations: The curse and blessing of multimodal posteriors, 2020.
- Zhang, Y., Apley, D. W., and Chen, W. Bayesian optimization for materials design with mixed quantitative and qualitative variables. *Scientific reports*, 10(1):1–13, 2020.

A. Experimental Setup

For the experimental setup, all the relevant methods are implemented as acquisition functions in BOTorch. For the active learning and for the BO experiments, we run NUTS (Hoffman & Gelman, 2014) in Pyro (Bingham et al., 2018). Tab. 1 displays the parameters of the MCMC in detail.

SAASBO experiments For the SAASBO experiments, we utilize Ax², which runs the BOTorch³ implementation of SAASBO with the default prior on the hyperparameters.

Additive Gaussian Process experiments The Additive GP setup closely resembles that of (Gardner et al., 2017). An additive partitioning is sampled, and the marginal likelihood of the model is maximized with regard to $\theta = \{\ell, \sigma_f, \sigma_\varepsilon\}$. We utilize a slightly adapted sampling scheme, and fix a maximal number of additive partitions. At each iteration of the MCMC scheme, two variables, sampled uniformly at random, are joined in a randomly assigned new group. We utilize the same warm-starting mechanism as described in Gardner et al. (2017), where at each iteration, the final accepted sample from the previous iteration acts as the initial proposal.

Task	Warmup	Thinning	No. hyperparameter sets	No. optima
Active Learning	256	16	100	N/A
BO - Synthetic	256	16	16	8
BO - GP samples	256	16	16	8
BO - SAASBO	128	8	16	8
BO - Additive GPs	32	8	12	8

Table 1. MCMC hyperparameters for all experiments.

A.1. GP Hyperparameters

Throughout the experiments, we primarily employed one prior: the $\mathcal{LN}(0, 3)$ prior on standardized inputs that was used in Riis et al. (2022). Furthermore, we consider the mean constant c as a learnable parameter in the BO experiments, with a conventional $\mathcal{N}(0, 1)$ prior on the standardized inputs.

A.2. Benchmarks

For the active learning benchmarks, we follow Riis et al. (2022) in the types of benchmarks and noise levels used. Each benchmark, as well as its search space, dimensionality and noise level is described in Tab. 2 and Tab. 3 for AL and BO, respectively. The noise level for all of the BO synthetic test functions were set to $\sigma_\varepsilon = 0.5$, except the Rosenbrock benchmarks, where the noise was set to $\sigma_\varepsilon = 2.5$, since the *normalized* noise variance would otherwise become low (roughly as low as 10^{-9} due to the extremely large output range of Rosenbrock) to the point of JES becoming unstable.

Task	Dimensionality	σ_ε	Search space
Gramacy	1	0.1	[0.5, 2.5]
Higdon	1	0.1	[0, 20]
Gramacy	2	0.05	$[-2, 6]^D$
Branin	2	11.32	$[-5, 10] \times [0, 15]$
Ishigami	3	0.187	$[-\pi, \pi]^D$
Hartmann-6	6	0.0192	$[0, 1]^D$

Table 2. Benchmarks used for the active learning experiments.

Compute resources. All experiments are carried out on *Intel Xeon Gold 6130* CPUs. Each repetition of the synthetic tasks are run on 4 cores, and the MLP tasks on 8 cores. Approximately 5,000 core hours each are used for the AL synthetic tasks, 10000 for the BO synthetic tasks, and 10000 for each self-correcting practical task.

²<https://github.com/facebook/Ax>

³<https://github.com/pytorch/botorch>

Task	Dimensionality	σ_ϵ	Search space
Branin	2	0.5	$[-5, 10] \times [0, 15]$
Rosenbrock-2	2	2.5	$[-1.5, 1.5]^D$
Hartmann-3	6	0.5	$[0, 1]^D$
Rosenbrock-4	4	2.5	$[-1.5, 1.5]^D$
Hartmann-4	4	0.5	$[0, 1]^D$
Hartmann-6	6	0.5	$[0, 1]^D$

Table 3. Benchmarks used for the Bayesian optimization experiments.

B. Additional Experiments

B.1. Marginal Likelihood Performance

We display the MLL performance of the various active learning acquisition functions. The MLL provides a measure of how accurate and *calibrated*, in terms of predictive uncertainty, the predictions of the model are. All acquisition functions struggle to achieve stable predictions throughout, which indicates a difficulty in finding stable and correct hyperparameters.

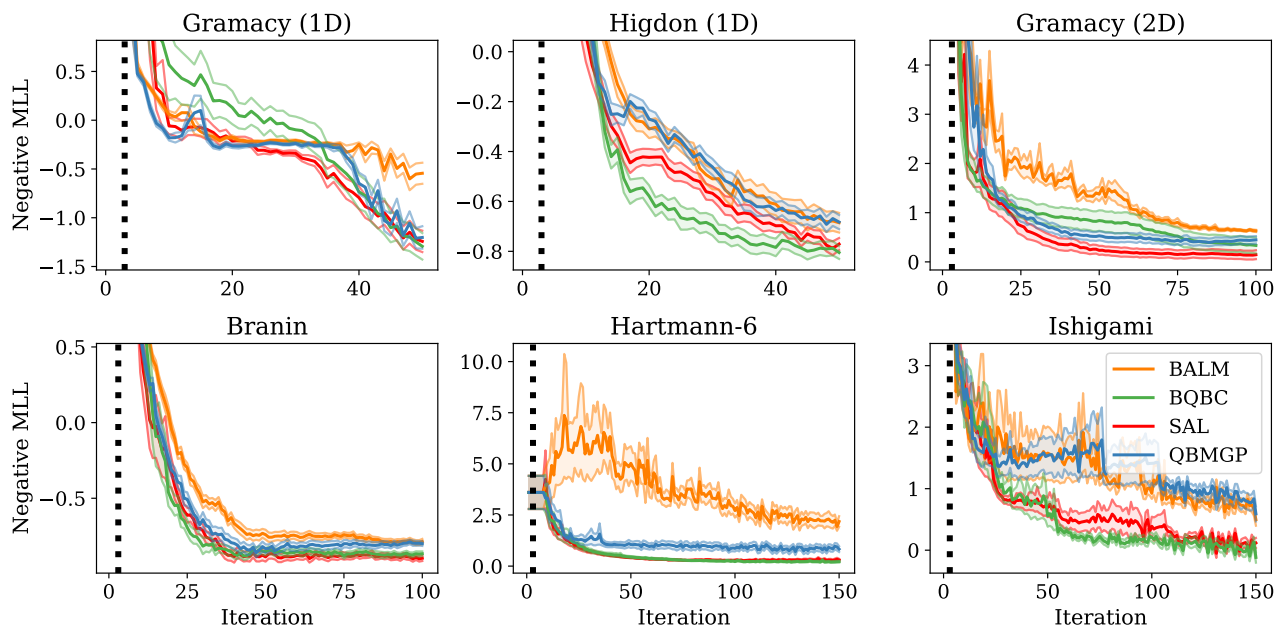


Figure 10. Negative marginal log likelihood (MLL) of the benchmarked active learning acquisition functions on the synthetic active learning tasks. The MLL is very unstable for two tasks, primarily due to hyperparameter uncertainty, but SAL and BQBC maintain the most consistent predictions throughout.

B.2. SAL Distance Measure Comparison

We show the performance of the statistical distance measures on the active learning tasks. These distances measure appreciate different quantities when the divergence is computed, where WS leans more towards global variance reduction - a generally good trait for active learning (MacKay & Neal, 1994). HS, however, emphasizes hyperparameter learning, which leads to more stable predictions, but occasionally insufficient exploration. As such, the RMSE of SAL-HR is non-competitive on many tasks. However, it substantially outperforms all other methods on MLL for Ishigami, which is caused by substantially better hyperparameter learning, which is evidenced in Fig. 14.

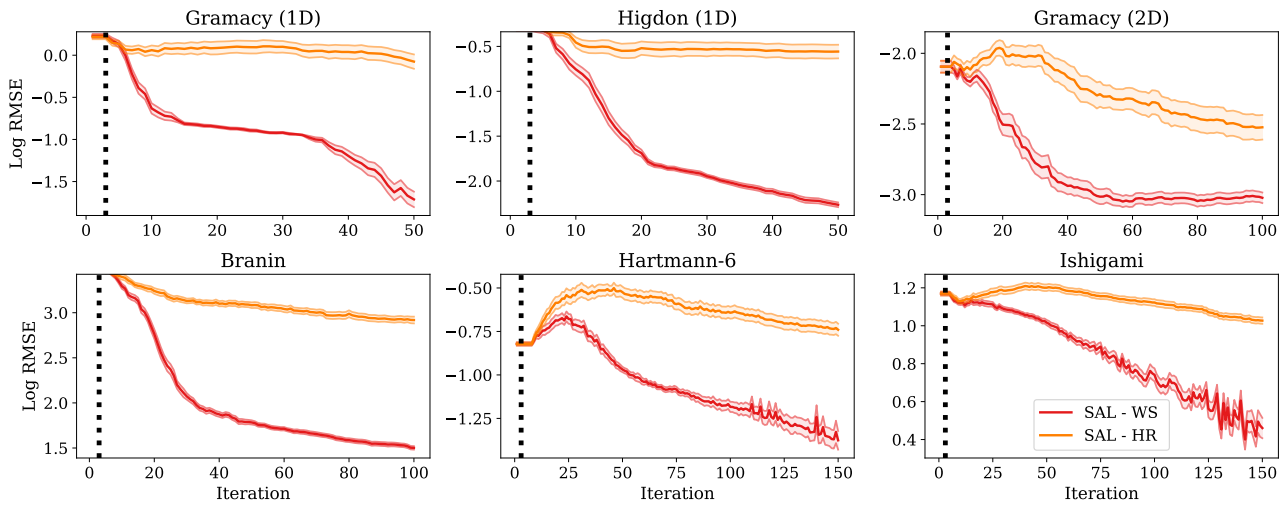


Figure 11. Log Regret of the Hellinger and Wasserstein MM-variants of SAL. SAL-HR is non-competitive on some benchmarks due to insufficient exploration of the search space.

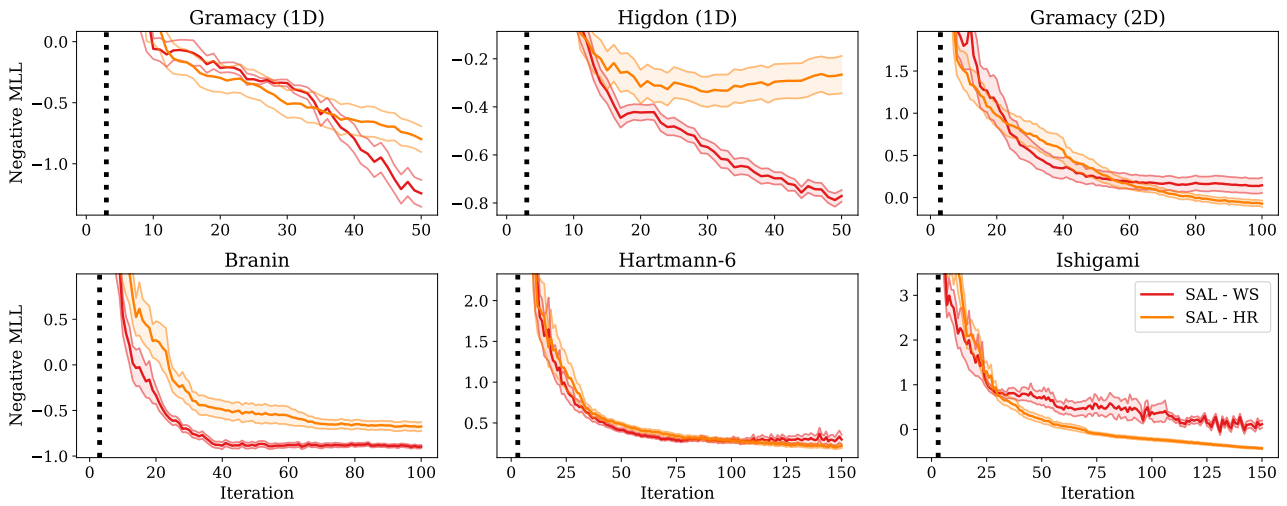


Figure 12. Log Regret of the Hellinger and Wasserstein MM-variants of SAL. SAL-HR is non-competitive on some benchmarks, but achieves drastically better and more stable predictions than all other benchmarks on Ishigami and Gramacy-2.

B.3. SCoreBO Distance Measure Comparison

We compare the Hellinger and Wasserstein variants of SCoreBO, both utilizing the MC approximation of the statistical distance. We note that SCoreBO-WS outperforms SCoreBO-HR on two tasks, but SCoreBO-HR is the overall more consistent approach. We hypothesize that the relative failure of SCoreBO-WS on Rosenbrock-4 is caused by its non-stationary structure, which likely causes exceedingly large exploration of the hyperparameter space.

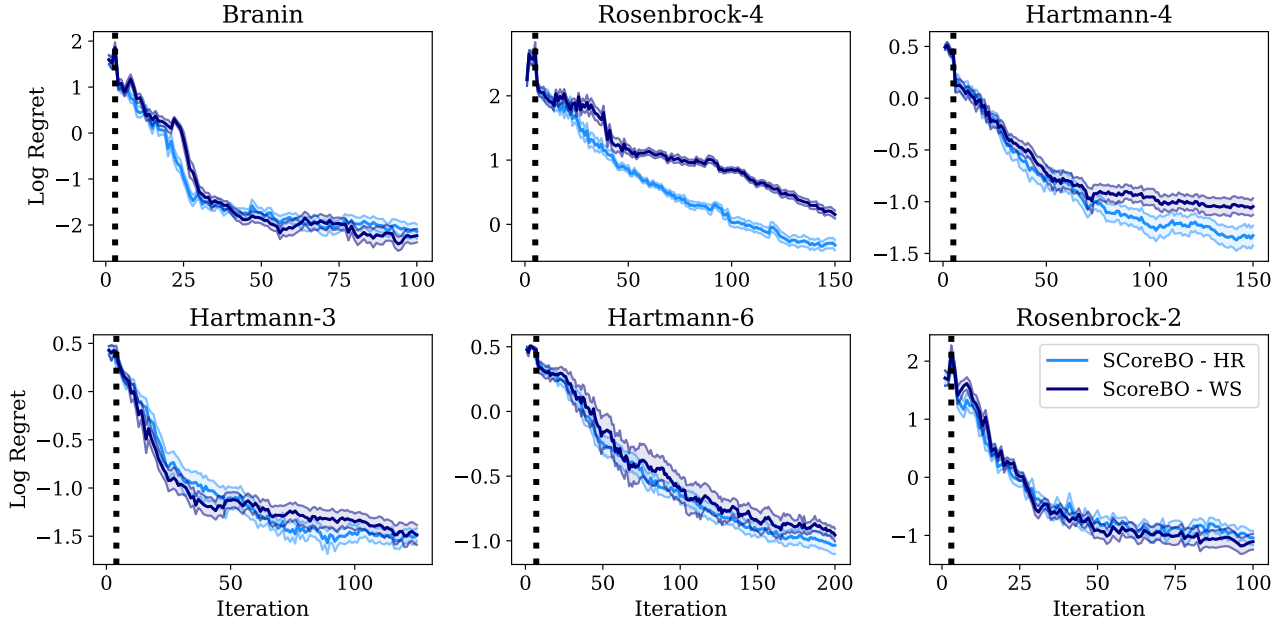


Figure 13. Log Regret of the Hellinger and Wasserstein MC-variants of SCoreBO. Both variants are competitive on all benchmarks, except for Wasserstein on Rosenbrock-4 which lags behind slightly. Overall, Hellinger is more consistent, and wins 4 out of 6 benchmarks.

C. Hyperparameter convergence

C.1. Active Learning Tasks

We display the hyperparameter convergence of SAL-WS, SAL-HR and the competing active learning acquisition functions. Both variants display accelerated hyperparameter learning compared to BQBC. , SAL-HR in particular achieves low-variance hyperparameter uncertainty on Ishigami and the higher-dimensional Hartmann-6, where other methods struggle. We obtain approximately correct hyperparameters for these tasks by randomly sampling 500 points on the noiseless benchmark, thereafter performing MCMC and averaging the sampled hyperparameter estimates in logspace. The noise level is known a priori. and estimates the other hyperparameters with substantially greater certainty than other methods.

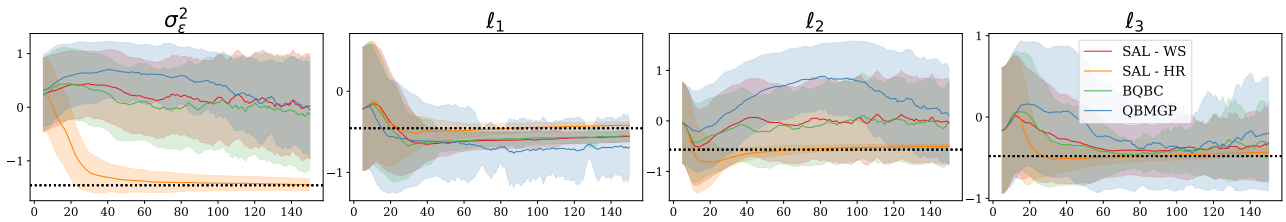


Figure 14. Hyperparameter convergence on the Ishigami test function. SAL-HR displays substantially more stable hyperparameter convergence than other approaches, and is the only acquisition function to accurately estimate the noise.

C.2. GP sample tasks

We display the convergence of SCoreBO and EI with a wide lognormal and BOTorch prior on the GP sample task. We observe that the lognormal prior is well-aligned for most hyperparameters, whereas BOTorch prior is misaligned. This is evidenced by the unimportant dimensions ℓ_6, ℓ_7 , and ℓ_8 , which have suggested lengthscales that are incorrect by more than an order of magnitude. Nevertheless, SCoreBO suggests lengthscales that are approximately twice as long ($10^{0.25}$) as EI ($10^{-0.05}$), and thus avoids unnecessary exploration along these dimensions. Moreover, SCoreBO correctly identifies the most important dimensions ℓ_1, ℓ_2 , and ℓ_3 with good accuracy quickly, whereas EI struggles to identify ℓ_1 . SCoreBO slightly overestimates the importance of dimensions 2 and 3, likely to compensate for the inability to accurately estimate the importance of other hyperparameters.

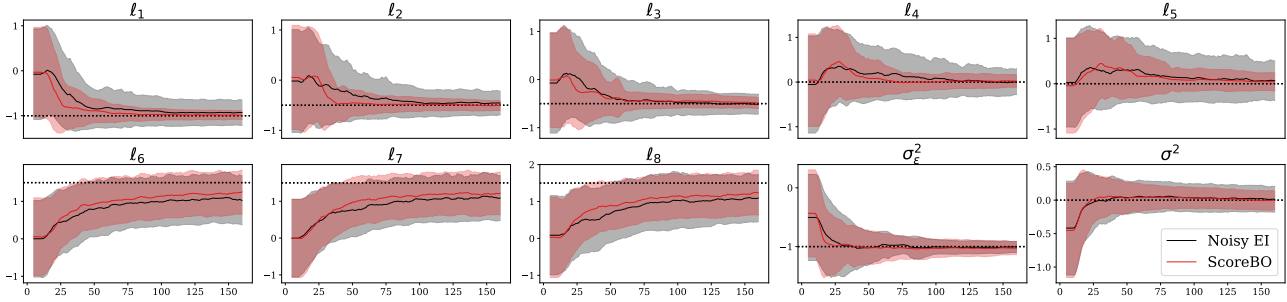


Figure 15. Hyperparameter convergence on the 8-dimensional GP sample for the broad log-normal prior. The black dashed line indicates true hyperparameter values. Mean and standard deviation are plotted across 20 repetitions, and a 3 iteration moving average of the plotted moments is applied to increase readability. Lengthscales ℓ_d ordered smallest (most important) to largest (least important). SCoreBO finds accurate hyperparameters faster, has the most accurate values for all hyperparameters, and has substantially lower variance for all important (i.e. not ℓ_6, ℓ_7 , and ℓ_8) hyperparameters except for the noise variance.

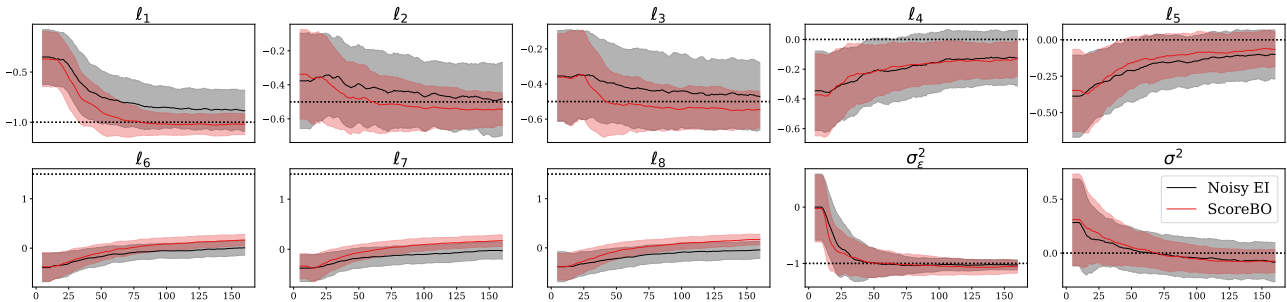


Figure 16. Hyperparameter convergence on the 8-dimensional GP sample for the BoTorch priors. The black dashed line indicates true hyperparameter values. Mean and standard deviation are plotted across 20 repetitions, and a 3 iteration moving average of the plotted moments is applied to increase readability. Lengthscales ℓ_d ordered smallest (most important) to largest (least important). SCoreBO finds accurate hyperparameters faster, has the most accurate values for all hyperparameters, and has substantially lower variance for all important (i.e. not ℓ_6, ℓ_7 , and ℓ_8) hyperparameters except for the noise variance.

C.3. Hyperparameter Divergence on Synthetic BO tasks

We highlight additional examples on synthetic BO test functions where hyperparameters diverge. Due to the non-stationary structure of Rosenbrock in particular (and to a lesser extent, Branin), hyperparameters values diverge as the number of observations increase. In particular, the extreme steepness along the edges suggests an exceedingly large outputscale. With increasing observations, a lengthscale-outputscale trade-off occurs, where both hyperparameters grow seemingly indefinitely. Notably, this behavior is consistent regardless of the acquisition function (BO, AL, SOBOL). Due to the restricted hyperparameter set employed in the AL tasks, this problem is distinct to the BO tasks.

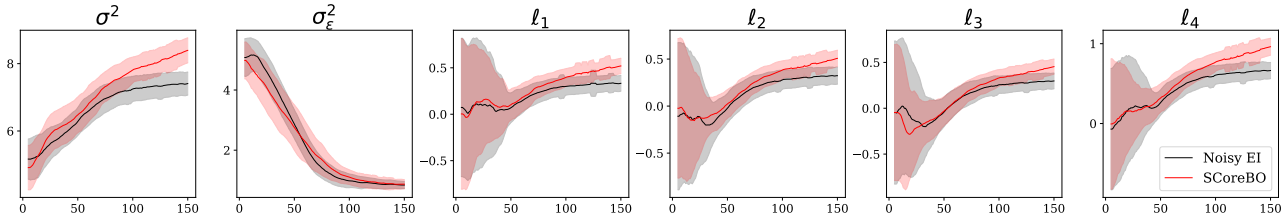


Figure 17. Hyperparameter divergence for SCoreBO and EI on Rosenbrock-4. The outputscale grows larger with increasing iterations, and the lengthscales grow similarly large as a countermeasure.

D. Approximation Strategies

We display the quality of the moment matching approximation for both the Hellinger and Wasserstein distance. Moreover, we compare the performances of the MM and MC approaches.

D.1. Performance of Monte Carlo

We display the performance of the MC variants of SAL-WS and SCoreBO-HR compared to their MM counterparts. Overall, performances are comparable, as each variant slightly exceeds the other on a couple of benchmarks. On the most complex benchmarks (Ishigami, Hartmann-4, Hartmann-6), the MC variant outperforms MM slightly, which suggests that MC is increasingly justified as disagreement in the posterior gets larger.

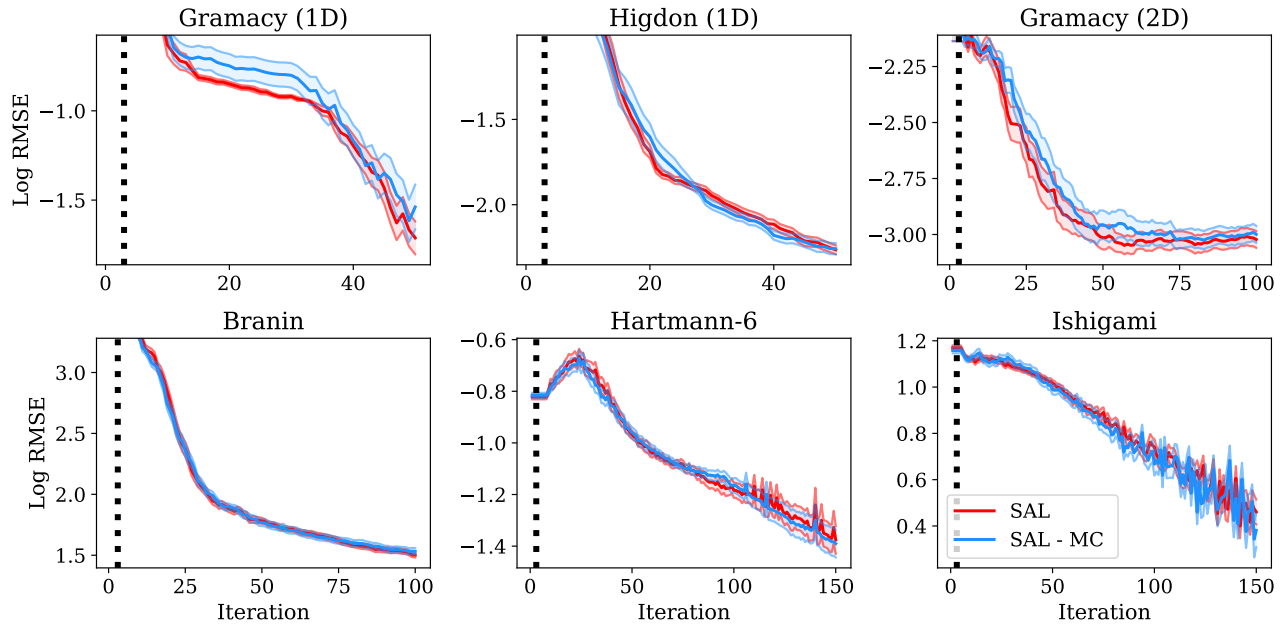


Figure 18. Log root mean squared error (RMSE) of the SAL MC (blue) and MM (red) variants on the active learning benchmarks. Overall performance is comparable, with the variants effectively tying all benchmarks. MC notably outperforms slightly on the difficult Ishigami test function.

D.2. Hellinger Distance Approximation

We display the accuracy of the moment matching approximation, and the sensitivity of the MC approximation to the number of samples L . In Fig. 23 and Fig. 24, we highlight two examples of the moment matching approximation in comparison to a large-scale, asymptotically exact variant of the MC approximation with 2048 samples. In Fig. 23, the MM approximation struggles to capture the sharp, multimodal surfaces in (blue), and consistently overestimates the distance in (orange). In

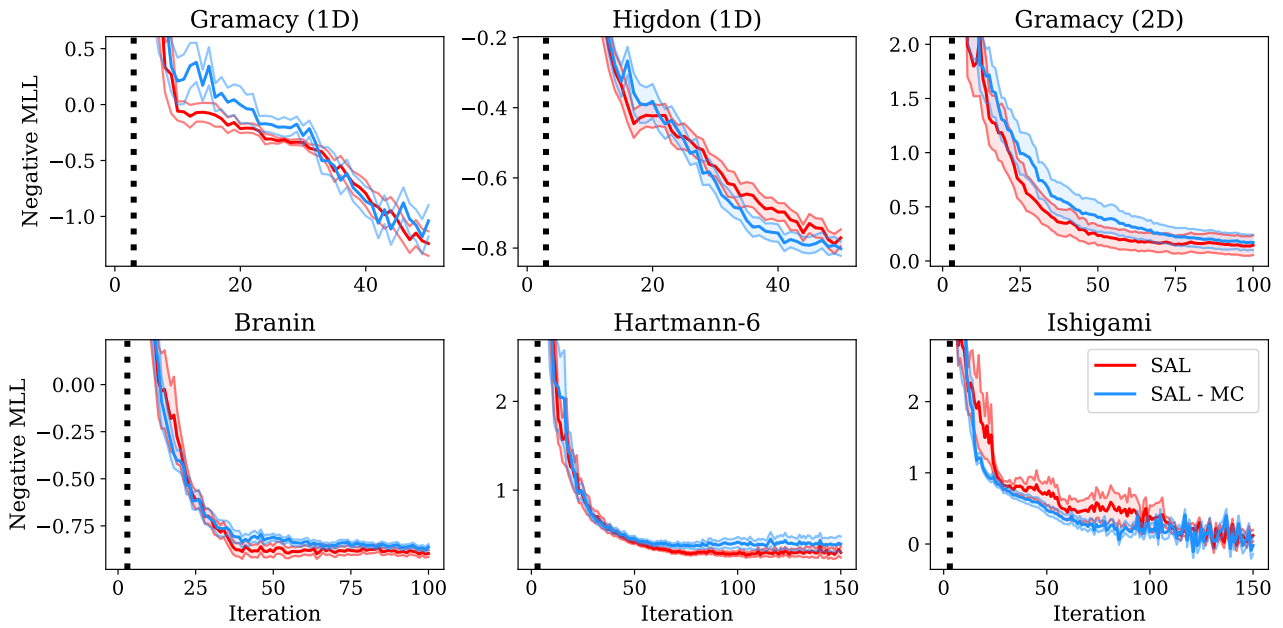


Figure 19. Negative marginal log likelihood (MLL) of the SAL MC (blue) and MM (red) variants on the active learning benchmarks. Overall performance is comparable, with three effectively tied benchmarks. MC outperforms slightly Hartmann-4 and Hartmann-6, and MM on Hartmann-3.

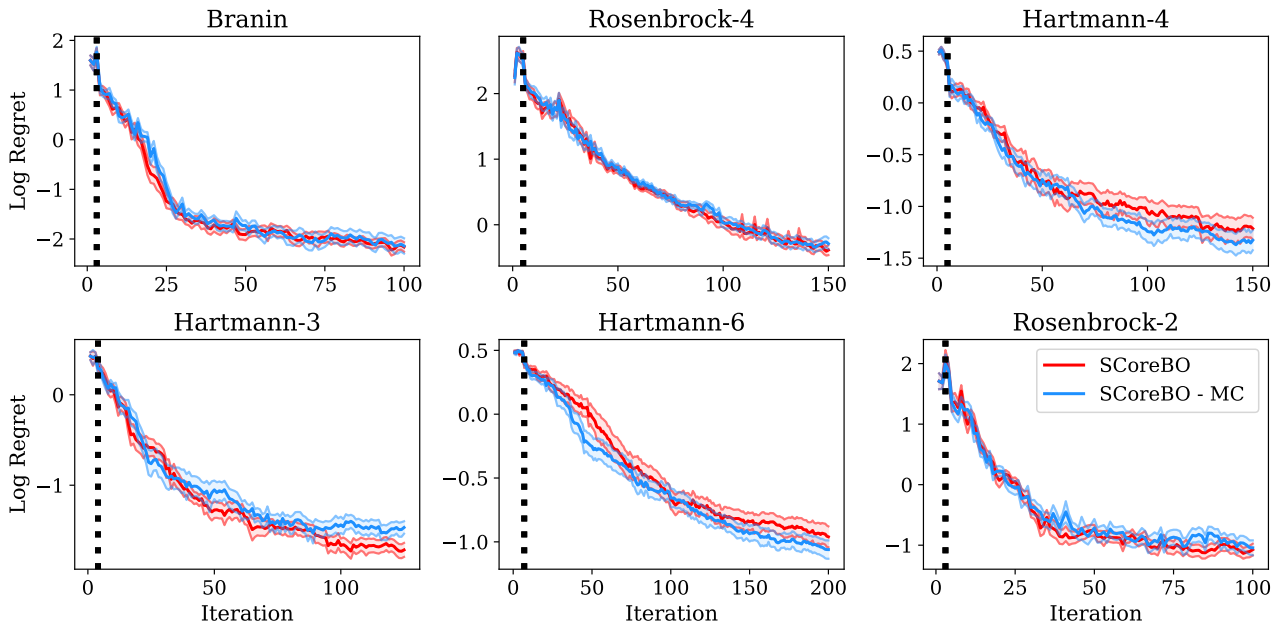


Figure 20. Log regret of SCoreBO-MM and SCoreBO-MC on the synthetic BO benchmarks. Overall performance is comparable, with MM outperforming marginally on 4 out of 6 tasks. MC notably outperforms slightly on the difficult Ishigami test function.

Fig. 24, the included conditional posteriors are substantially more similar, and as such, the moment matching approximation is more accurate. The shape of the acquisition function is captured almost perfectly, and the magnitude is only marginally overestimated, most prominently in (green). We display the

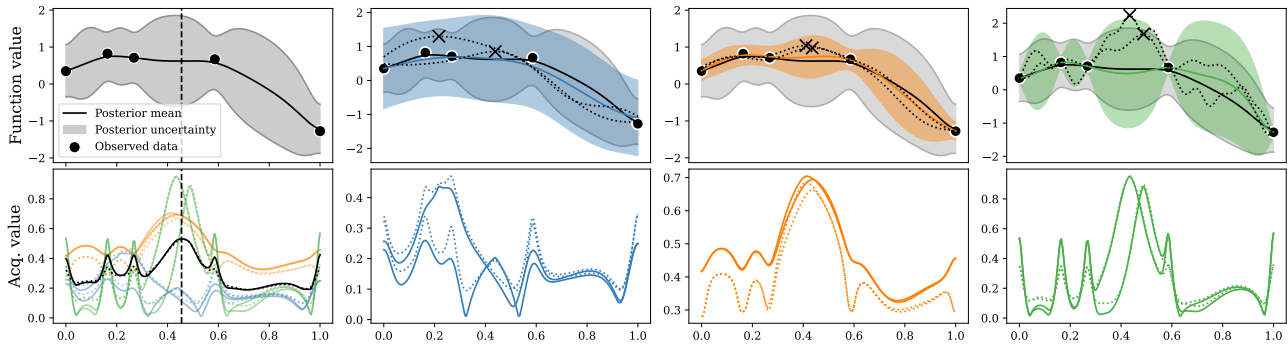


Figure 21. Example of the per-sample Hellinger distance computation using moment matching (solid lines) and large-scale, asymptotically exact quasi-MC with 2048 samples. The moment matching approximation mostly retains the shape of the asymptotically exact variant. However, it does not perfectly capture the multi.modality in (blue), and overestimates the distance in the low-variance region at the right edge of (orange). The acquisition function y-axis is scaled individually per model to better highlight the difference in acquisition function value.

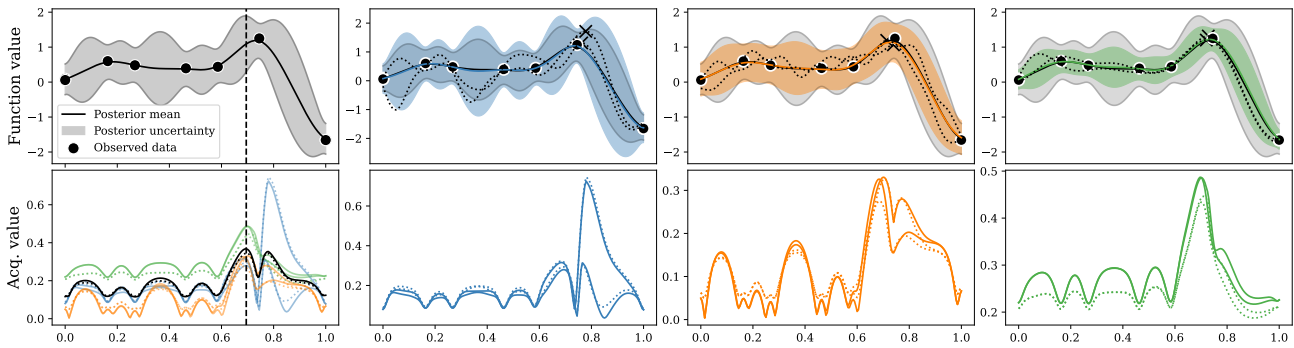


Figure 22. Example of the per-sample Hellinger distance computation using moment matching (solid lines) and large-scale, asymptotically exact quasi-MC with 2048 samples. The moment matching approximation captures the shape of the asymptotically exact variant well, but overestimates the distance slightly in (green). The acquisition function y-axis is scaled individually per model to better highlight the difference in acquisition function value.

D.3. Wasserstein Distance Approximation

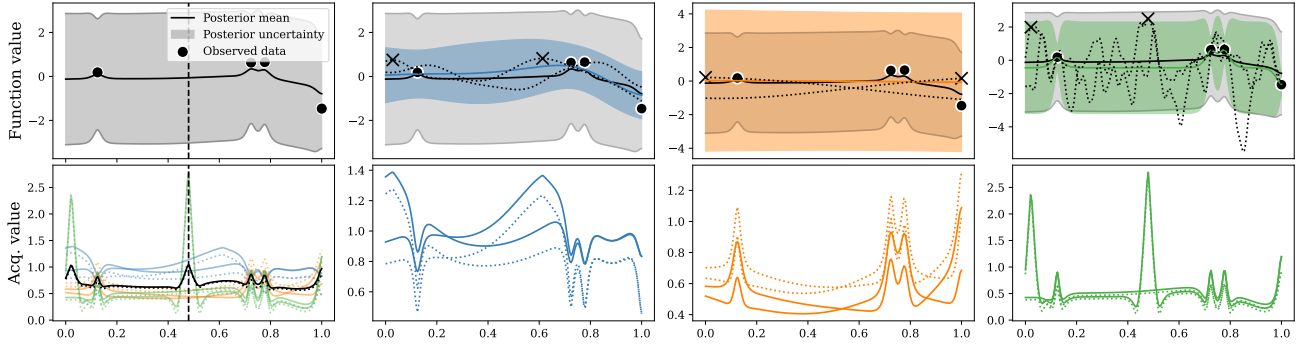


Figure 23. Example of the per-sample Wasserstein distance computation using moment matching (solid lines) and large-scale, asymptotically exact quasi-MC with 2048 samples. The moment matching approximation mostly retains the shape of the asymptotically exact variant. The shape of the acquisition function is generally well captured, but high-variance regions have their distance underestimated by the moment matching approach, and low-variance regions have their distance over-estimated, leading to a biased approximation. The acquisition function y-axis is scaled individually per model to better highlight the difference in acquisition function value.

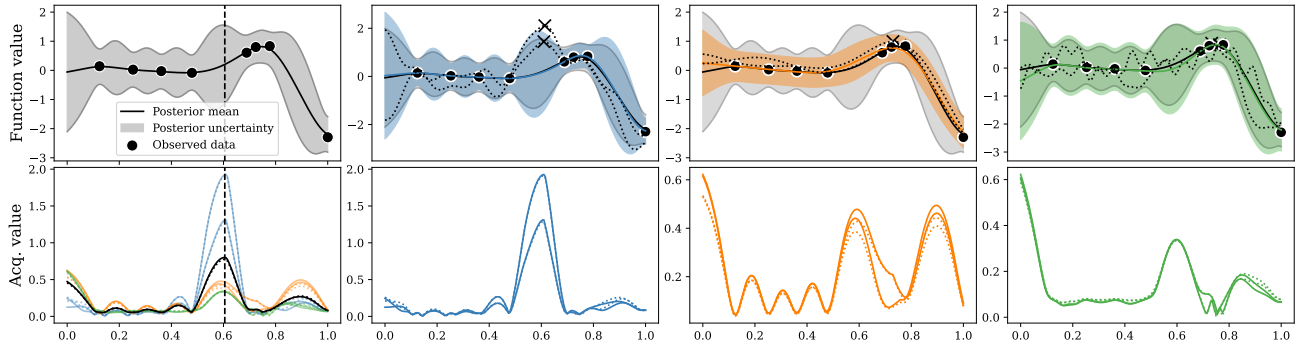


Figure 24. Example of the per-sample Wasserstein distance computation using moment matching (solid lines) and large-scale, asymptotically exact quasi-MC with 2048 samples. The moment matching approximation captures the shape of the asymptotically exact variant well, and only marginally over- and underestimates the distance. The acquisition function y-axis is scaled individually per model to better highlight the difference in acquisition function value.